A fixed-target programme at the LHC (AFTER@LHC)

Barbara Trzeciak, on behalf of the AFTER@LHC study group [1]
Utrecht University, Princetonplein 1, 3584 CC Utrecht, The Netherlands

E-mail: b.a.trzeciak@uu.nl

Abstract. We report on the perspectives for hadron, heavy-ion and spin physics with a multi-purpose fixed-target programme using the LHC multi-TeV proton and heavy-ion beams (AFTER@LHC). This would be the most energetic fixed-target experiment opening new domains of particle and nuclear physics and complementing current and future collider programmes. Thanks to the large boost, one can fully access –with conventional detectors– the backward hemisphere in the center-of-mass system which allows for studies of the largely uncharted high-x region ($x_F \to$ -1).

1. Introduction

AFTER@LHC is a proposal for a multi-purpose fixed-target experiment using the multi-TeV proton and heavy-ion beams of the LHC [1, 2, 3]. The physics cases of such an experiment covers 3 main fields : (i) the understanding of the high-x gluon, antiquark and heavy-quark content in the nucleon and nucleus; (ii) the dynamics and spin of gluons inside (un)polarised nucleons; (iii) heavy-ion collisions from mid to large rapidities between SPS and RHIC energies.

The most relevant advantages of a fixed-target mode compared to a collider mode are: (1) an easy access to high Feynman $|x_F|$ domain by studying the far backward region in the center-of-mass system (c.m.s); (2) the versatility of the target species; (3) the possibility to polarise a target; (4) the very high luminosities with either dense targets or high intensity beams. All this can be realized in a setup not affecting the LHC performance itself.

With the 7 TeV proton beam colliding on a fixed target, the c.m.s energy per NN collisions ($\sqrt{s_{NN}}$) is 115 GeV, with a rapidity shift $\Delta y^{\rm lab}_{\rm c.m.s} \approx 4.8$ ($y_{\rm c.m.s} = 0 \to y_{\rm lab} = 4.8$). The 2.76 TeV Pb beam provides $\sqrt{s_{NN}} \approx 72$ GeV and the rapidity shift of 4.3. This gives the same c.m.s energy for $p+p$, $p+d$, $p+A$ collisions with the LHC proton beam, and for Pb+p, Pb+A collisions with the LHC lead beam. Due to the large boost, the entire forward hemisphere, $y_{\rm c.m.s} > 0$, falls within an angle of $0^\circ < \theta_{\rm lab} < \mathcal{O}(1^\circ)$ w.r.t to the beam axis in the laboratory frame. Due to the large occupancy, the forward region is challenging to access. On the contrary, the backward hemisphere, $y_{\rm c.m.s} < 0$, corresponds to larger angles in the laboratory frame and is easily accessible using standard detection techniques without the need to cope with constraints from the beam pipe. This provides an access to the largely uncharted backward physics with partons having a momentum fraction $x_2 \to 1$ in the target ($x_F \to$ -1), for different systems.

Several technological options allowing one to perform fixed-target experiments with the LHC beams are currently under investigation: (1) installing an internal gas target [4, 5, 6]; (2) placing a wire target in the beam halo [7]; (3) deviating a part of the beam halo with a bent-crystal onto an external target [8, 9]. The advantages of the first option is the possibility of combining it with an existing detector, such as LHCb or ALICE. Furthermore, by installing a HERMES-like Storage Cell [10] as a target, polarised gases can be used such that an ambitious spin-physics

[1] M. Anselmino, R. Arnaldi, S.J. Brodsky, V. Chambert, C. Da Silva, J.P. Didelez, M.G. Echevarria, E.G. Ferreiro, F. Fleuret, Y. Gao, B. Genolini, C. Hadjidakis, I. Hřivnáčová, D. Kikola, A. Klein, A. Kurepin, A. Kusina, J.P. Lansberg, P. Lenisa, F. Lyonnet, L. Massacrier, C. Lorcé, A. Nass, C. Quintans, F. Rathmann, P. Robbe, I. Schienbein, E. Scomparin, J. Seixas, H.S. Shao, A. Signori, E. Steffens, N. Topilskaya, U.I. Uggerhøj, R. Ulrich, Z. Yang.

program can be conducted. The bent-crystal option can be used in two ways: (i) with a dedicated beamline which is probably the most costly option; (ii) keeping the particles deviated by the bent crystal inside the beampipe as a split beam which would then interact with a target adapted to the beampipe. Further investigations are needed to tell whether this beam splitted option is compatible with a polarised target like that of [11] and the use of LHCb or ALICE.

2. Physics highlights and projection studies

2.1. Set-up for projection studies

The simulations presented here focus on quarkonium and Drell-Yan (DY) production by exploring di-muon ($\mu^+\mu^-$) pair production from different sources. The signal (quarkonia and DY) and different di-muon background sources are separately studied in order to keep a good control over the input distributions and the normalization of these different sources. The quarkonium signal, DY and correlated open-charm and beauty backgrounds ($c\bar{c}, b\bar{b}$) were simulated with HELAC-Onia [12, 13]. The events were processed with Pythia 8 [14] to perform the hadronisation, to account for initial/final-state radiations and for the decay of resonances. The uncorrelated background (mostly μ coming from pion and kaon decays) was obtained from minimum bias $p + p$ collisions generated with Pythia 8. Afterwards, a fast simulation was performed to account for realistic detector-resolution and particle-identification performances. The detector response –momentum resolution, μ identification efficiency and π/K misidentification probability with μ– was simulated with a detector setup similar to the LHCb detector [15] with a pseudorapidity coverage of $2 < \eta_{\rm lab} < 5$. More details on the applied procedure can be found in Ref. [16]. First projections for $p+A$ and $A+A$ collisions are done by applying a scaling factor to $p+p$ simulations, with no nuclear effects considered (not even isospin corrections). For the quarkonium and DY simulations, where the full background is considered, the uncorrelated one is subtracted only assuming the like-sign technique (that is, the worst case scenario in terms of the expected statistical uncertainties). Integrated luminosities taken for the simulations and expected to be achieved within one year are: $p + p$: 10 fb^{-1}, $p + A$: 100 pb^{-1} and $A + A$: 7 nb^{-1}.

2.2. QCD and nuclear PDFs (nPDFs) studies at high x with a proton beam

Among the goals of AFTER@LHC are high-x studies for particle and astroparticle physics. The most relevant features of AFTER@LHC in this case are the very high luminosities, the access towards very low p_T and backward rapidities; it would indeed be a multi-purpose experiment providing detailed studies of heavy-flavour, quarkonia and prompt photon production. In order to solve long standing debates in quarkonium hadroproduction (see [17]), precise measurements of cross-sections, correlations and polarisations of *a large number of* quarkonium states are essential. Such measurements can be conducted at AFTER@LHC thanks to the large expected quarkonium yields – typically 10^9 for charmonia and 10^6 for bottomonia over a year accounting for the branchings. AFTER@LHC will also give a unique opportunity to access C-even quarkonia ($\chi_{c,b}, \eta_c$) and associated-production channels [18] in a new energy and rapidity domain. In $p+p$ and $p + A$ collisions, quarkonium studies can be performed over wide transverse momenta and rapidities beyond that of RHIC experiments [16].

Thanks to the access to the target-rapidity region, the gluon, antiquark and heavy-quark distributions in the proton, neutron and nuclei can then be extracted at mid- and high-momentum fractions x. The wide rapidity coverage will help to study nuclear effects in the antishadowing, EMC and Fermi motion regions (essentially $x_2 > 0.05$). The search of a possible *gluon* EMC effect could be crucial to understand the origin of the quark EMC effect and its connections with short-range correlations in nuclei. Furthermore, a precise knowledge of nPDFs is important for studies of heavy-ion collisions as fundamental inputs for the initial states of the collisions. In [16, 21], the impact of the gluon densities on the nuclear modification factors of prompt and non-prompt J/ψ and Υ in p+Pb and Pb+Pb was evaluated using the EPS09 parametrization. The effect of coherent energy loss was also studied in [22]. An example of the

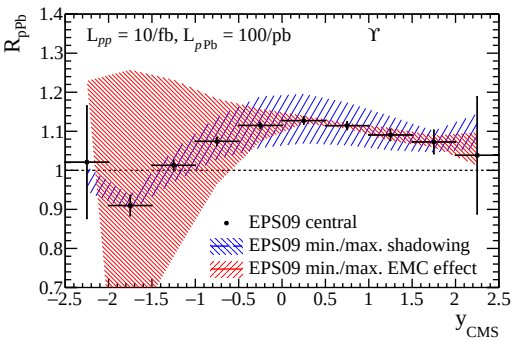

Figure 1. Nuclear modification factor for Υ vs. $y_{\text{c.m.s.}}$ in p+Pb collisions at $\sqrt{s_{NN}}$ = 115 GeV (from [16]). Points represent EPS09 [19] central prediction with statistical uncertainties based on expected yields at AFTER@LHC. Uncertainties of the nPDF in EPS09 assuming min./max. shadowing and min./max. EMC effect are shown as the blue and red band, respectively.

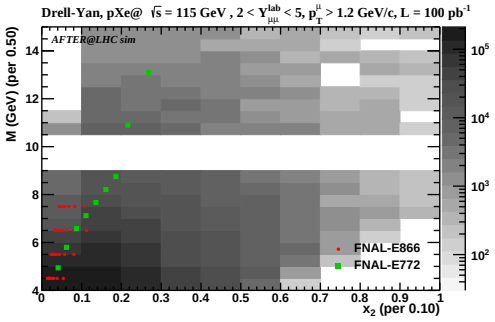

Figure 2. DY yields in the di-muon invariant mass (excluding Υ states region) and x_2 bins in p+Xe collisions with existing DY $p + A$ data used for nPDF fits [20] – p+Xe at $\sqrt{s_{NN}}$ = 115 GeV.

nPDF uncertainties propagated to Υ R_{pA} is given on Figure 1 and is compared to projected experimental uncertainties, which are much smaller in the ALICE and LHCb y acceptance.

nPDFs can be further constrained by DY measurements. Figure 2 shows the huge expected DY yields as a function of the di-muon invariant mass and x_2 in p+Xe collisions – similar yields are expected for $p + p$ collisions. The existing DY $p + A$ data currently used for global nPDF fits are also shown in red and green (see [20]). It is obvious that AFTER@LHC offers a unique coverage towards the unexplored high x region in $p + A$ with extremely high yields (in $p + p$, $p + A$). The expected precision on a nuclear modification factor (R_{pXe}) measurement is presented in Figure 3 for 3 rapidity bins corresponding to different x_F ranges. The statistical uncertainties are dominated by uncertainties from the uncorrelated background subtraction with like-sign techniques. These could probably be reduced using event mixing down to a level where systematical uncertainties would then become dominant. We stress that going to the very backward rapidities ($2 < y_{\text{lab}} < 3$) –which probably is the most interesting one physics wise, renders the DY signal even more clean since the quark-induced processes are favoured and the background is reduced accordingly.

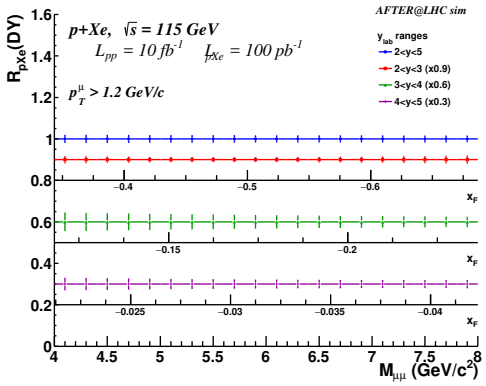

Figure 3. Statistical precision on the DY $R_{p\text{Xe}}$ *vs* di-muon invariant mass (and x_F) for 3 rapidity ranges – p+Xe at $\sqrt{s_{NN}}$ = 115 GeV.

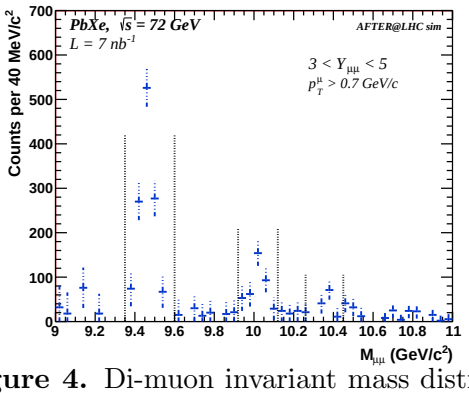

Figure 4. Di-muon invariant mass distribution in the Υ(nS) region. The uncorrelated background was subtracted through the like-sign technique – Pb+Xe at $\sqrt{s_{NN}}$ = 72 GeV.

Giving the large expected yields, one can also measure the single spin asymmetries (A_N) for all quarkonia states and DY with unheard of precision and quantify the gluon and quark Sivers effects. For more insights into the spin physics opportunities, see [23, 24, 25, 26, 27].

2.3. Physics highlights for heavy-ion collisions

One of the prime objectives of heavy-ion physics at high-energy facilities is the search and characterisation of the Quark-Gluon Plasma (QGP). AFTER@LHC with $\sqrt{s_{NN}} = 72$ GeV provides a complementary coverage to the RHIC and SPS experiments in a temperature and baryon chemical potential region where the QGP is expected to be formed. Thanks to the aforementioned assets of the fixed-target mode, the longitudinal expansion of the hot medium can be studied using the wide available rapidity coverage with colliding systems of different sizes with the LHC Pb beam. With the rapidity scan one can probe the medium at different average temperatures and energy densities and infer the temperature dependence of the shear viscosity of the QGP liquid [28]. In addition, one can perform precise measurements of the QGP properties with hard probes. Figure 4 shows expected $\Upsilon(nS)$ yields in Pb+Xe collisions with a excellent separation of the 3 Υ states. What is also important for hot-medium investigations is the target versatility since it offers a unique opportunity to study the cold nuclear matter effects and their factorization. The ideal probe for such checks is DY as it is immune from the final state QCD matter effects in AB collisions. AFTER@LHC is probably the only facility where this can be done. Finally, precise charm and beauty measurements will address the long standing question of heavy-quark energy loss in the medium [29] - collisional *vs* radiative energy loss.

3. Conclusions

We have reported on the proposal of performing fixed-target experiments with the multi-TeV LHC proton and lead beams. We have presented a selection of physics topics with projection studies. Such a new experimental endeavour opens the way to a number of unique and precise measurements, many of which can not be performed elsewhere, significantly advancing our knowledge in the fields of heavy-ion, hadron, spin and astroparticle physics.

References

[1] S. J. Brodsky, F. Fleuret, C. Hadjidakis, J. P. Lansberg, *Phys. Rept.* **522**, 239 (2013).
[2] J. P. Lansberg, S. J. Brodsky, F. Fleuret, C. Hadjidakis, *Few Body Syst.* **53**, 11 (2012).
[3] J. P. Lansberg, *et al.*, *PoS* **QNP2012**, 049 (2012).
[4] C. Barschel, Ph.D. thesis, RWTH Aachen U. CERN-THESIS-2013-301 (2014).
[5] M. Ferro-Luzzi, *Nucl. Instrum. Meth.* **A553**, 388 (2005).
[6] R. Aaij, *et al.*, *JINST* **9**, P12005 (2014).
[7] A. B. Kurepin, N. S. Topilskaya, *Adv. High Energy Phys.* **2015**, 760840 (2015).
[8] W. Scandale, *ECFA LHC Workshop, Aachen, Germany, October 4-9, 1990* (1990), pp. 760–764.
[9] E. Uggerhoej, U. I. Uggerhoej, *Nucl. Instrum. Meth.* **B234**, 31 (2005).
[10] C. Barschel, P. Lenisa, A. Nass, E. Steffens, *Adv. High Energy Phys.* **2015**, 463141 (2015).
[11] C. Brown, *et al.*, Letter of Intent for a Drell-Yan Experiment with a Polarized Proton Target (2014).
[12] H.-S. Shao, *Comput. Phys. Commun.* **184**, 2562 (2013).
[13] H.-S. Shao, *Comput. Phys. Commun.* **198**, 238 (2016).
[14] T. Sjostrand, S. Mrenna, P. Z. Skands, *Comput. Phys. Commun.* **178**, 852 (2008).
[15] A. A. Alves, Jr., *et al.*, *JINST* **3**, S08005 (2008).
[16] L. Massacrier, *et al.*, *Adv. High Energy Phys.* **2015**, 986348 (2015).
[17] A. Andronic, *et al.*, *Eur. Phys. J.* **C76**, 107 (2016).
[18] J.-P. Lansberg, H.-S. Shao, *Nucl. Phys.* **B900**, 273 (2015).
[19] K. J. Eskola, H. Paukkunen, C. A. Salgado, *JHEP* **04**, 065 (2009).
[20] K. Kovarik, *et al.*, *Phys. Rev.* **D93**, 085037 (2016).
[21] R. Vogt, *Adv. High Energy Phys.* **2015**, 492302 (2015).
[22] F. Arleo, S. Peigne, *Adv. High Energy Phys.* **2015**, 961951 (2015).
[23] M. Anselmino, U. D'Alesio, S. Melis, *Adv. High Energy Phys.* **2015**, 475040 (2015).
[24] K. Kanazawa, Y. Koike, A. Metz, D. Pitonyak, *Adv. High Energy Phys.* **2015**, 257934 (2015).
[25] T. Liu, B.-Q. Ma, *Eur. Phys. J.* **C72**, 2037 (2012).
[26] L. Massacrier, *et al.*, *Int. J. Mod. Phys. Conf. Ser.* **40**, 1660107 (2016).
[27] J. P. Lansberg, *et al.*, *EPJ Web Conf.* **85**, 02038 (2015).
[28] G. Denicol, A. Monnai, B. Schenke, *Phys. Rev. Lett.* **116**, 212301 (2016).
[29] D. Kikola, *Adv. High Energy Phys.* **2015**, 783134 (2015).